DESIGN AND DEVELOPMENT OF AN INSECT-INSPIRED MICRO AIR VEHICLE

CHEAW BOON HONG

SCHOOL OF AEROSPACE ENGINEERING
UNIVERSITI SAINS MALAYSIA
2019

DESIGN AND DEVELOPMENT OF AN INSECT-INSPIRED MICRO AIR VEHICLE

by

CHEAW BOON HONG

Thesis submitted in fulfilment of the requirements for the Bachelor Degree of Engineering (Honours) (Aerospace Engineering)

June 2019

ENDORSEMENT

I, Cheaw Boon Hong hereby declare that all corrections and comments made by the supervisor and examiner have been taken consideration and rectified accordingly.

_____

(Signature of Student)

Date:

_____

(Signature of Supervisor)

Name:

Date:

_____

(Signature of Examiner)

Name:

Date:

DESIGN AND DEVELOPMENT OF AN INSECT-INSPIRED MICRO AIR VEHICLE

ABSTRACT

Micro Air Vehicles (MAVs) are now an active research focus that has caught attention from global talents. With its' small size, MAVs have considerable potential to be capable of performing missions such as environmental monitoring, surveillance and assessment in hostile situation. Through the process of mimicking insect flight, however, researchers from both in educational institution and industry are facing a lot of challenges such as instability of the air vehicle during the hovering, the maneuverability, the propulsive efficiency due to miniaturization. The objective is to innovate an efficient four-winged FW-MAV platform with better payload carrying capability, where human can allocate important payloads on the FW-MAV during environmental monitoring and indoor surveillance missions. Using Computer Aided Design (CAD) software SolidWorks, the FW-MAVs' wing and tail are designed. With the allocated time and financial support, two wings are developed using traditional cut and glue method and advanced vacuum mold method. Avionics connection is tested before assembling with the wing and tail. Flight test and vertical thrust measurement are conducted on FW-MAV to compare the performance of different wings and different model at full throttle maximum speed. In general, the FW-MAV produces maximum vertical thrust at 10° angle of attack. Wing which has the stiffeners and manufactured using vacuum mold produces the highest thrust compare with other wings. Possible future work is to optimize the tail design and control algorithm in order to achieve hovering flight.

REKA BENTUK DAN PEMGEMBANGAN PESAWAT UDARA MIKRO BERINSPIRASI SERRANGGA

ABSTRAK

Pesawat Udara Mikro merupakan satu kajian aktif yang menarik perhatian secara global. Dengan saiznya yang kecil, Pesawar Udara Mikro mempunyai potensi untuk menjalani misi seperti pemantauan alam sekitar, pengawasan dan penilaian pada situasi bahaya. Melalui proses meniru penerbangan serangga, penyelidik dari institusi pendidikan dan industry telah menghadapi banyak halangan seperti pesawat yang tidak stabil waktu melayang, manuver dan kecekapan penggerak disebabkan saiznya yang kecil. Objektif projek adalah untuk menginovasi platform Pesawat Udara Mikro empat sayap yang cekap dengan keupayaan membawa muatan yang lebih, di mana manusia boleh memperuntukkan muatan yang penting atas Pesawat Udara Mikro empat sayap waktu pemantauan alam sekitar dan misi pengawasan dalaman. Dengan menggunakan perisian Computer Aided Design (CAD) iaitu Solidwork, reka bentuk sayap dan ekor Pesawat Udara Mikro empat sayap telah dihasilkan. Dengan masa yang diperuntukkan dan sokongan kewangan, dua sayap telah dibina dengan cara tradisional iaitu gunting dan gam dan cara maju iaitu cara acuan vakum. Sambungan avionic telah diuji sebelum digabungkan dengan sayap dan ekor pesawat yang telah dibina. Ujian penerbangan dan pengukuran tujah menegak telah dibuat untuk membandingkan prestasi sayap dan model yang berlainan pada pendikit penuh kelajuan maksimum. Secara amnya, Pesawat Udara Mikro menghasilkan maksimum tujah menegak pada sudut 10°. Sayap yang mempunyai pengeras dan dibina dengan menggunakan acuan vakum menghasilkan tujah menegak yang paling tinggi. Kemungkinan kerja yang boleh dibuat pada masa depan adalah mengoptimumkan reka bentuk ekor pesawat dan mengawal algoritma untuk mencapai penerbangan melayang.

ACKNOWLEDGEMENTS

This Final Year Project (FYP) will not be possible without the generous help and endless support from many individuals. I would like to express my gratitude to all of them. First of all, a million thanks to Dr. Ho Hann Woei for his guidance on solving difficult problems and his support which have made this project successful.

I appreciate time and effort given by the professional team of technicians from School of Aerospace Engineering. They are Mr. Ismail b. Mohamed Shorhami, Mr. Muhamad Zulkhairi bin Mat Saad, Mr. Mohd Amir bin Wahab, Mr. Hasfizan bin Hashim, Mr. Abdul Hisham bin Sulaiman, Mr. Mohd Shahar bin Che Had@Mohd Noh, and Mr. Mohd Najib bin Mohd Hussian for their kind co-operation and assistance on fabricating necessary parts and equipment for this project.

Last but not least, I am grateful to have extremely supportive friends, seniors, course mates and other respectful lecturers. Never forget the moral support and precious advice from these lovely people given during my time working on the project.

I will make full use of the project management, hands-on skills and engineering knowledge learnt from this final year project on my future project undertaking. I will always remember the aspiration of becoming a better engineer, innovate and improve things and make the world a better place.

DECLARATION

This thesis is the result of my own investigation, except where otherwise stated and has not previously been accepted in substance for any degree and is not being concurrently submitted in candidature for any other degree.

_____

(Signature of Student)

Date:

TABLE OF CONTENT

LIST OF FIGURES

LIST OF TABLES

LIST OF ABBREVIATIONS

MAV	: Micro Air Vehicle
UAV	: Unmanned Aerial Vehicle
DARPA	: Defense Advanced Research Project Agency
FW-MAV	: Flapping Wing Micro Air Vehicle
IMU	: Inertial Measurement Unit
NAV	: Nano Air Vehicle
PAV	: Pico Air Vehicle
AR	: Aspect Ratio
GR	: Gear Ratio
MOSFET	: Metal-oxide Semiconductor Field-Effect Transistor
MDF	: Medium-density Fibreboard
PET	: Polyethylene Terephthalate
LEV	: Leading Edge Vortex

LIST OF SYMBOLS

g	: Acceleration of gravity [m/s^2]
L_0	: Latitude [°]
h_0	: Altitude [m]
T_a	: Air temperature [°C]
ρ	: Air density [kg/m^3]
ν	: Kinematic viscosity [m^2]
p	: Air pressure [Pa]
h_0	: Altitude, m
T_{SL}	: Sea level thrust
e	: Oswald efficiency factor
U_{ref}	: local reference velocity [m/s]
U	: Velocity [m/s]
T/W	: Thrust loading
W/S	: Wing loading
W_{Str}	: Weight of structure [g]
W_{Eq}	: Weight of equipment [g]
W_{To}	: Total weight [g]
W_B	: Weight of battery [g]
W_{PL}	: Weight of payload [g]
W_{AV}	: Weight of avionics [g]
W_{PP}	: Weight of power plant [g]
W_{Wing}	: Weight of wing [g]
W_{Tail}	: Weight of tail [g]
$W_{Fuselage}$	: Weight of fuselage [g]
$W_{Mechanism}$	: Weight of mechanism [g]
W_{Other}	: Weight of wires and etc. [g]
S_w	: Total wing area [mm^2]
b	: Wingspan [mm]
AR_w	: Wing aspect ratio

λ : Tapered ratio

C_t : Tip chord length [mm]

C_r : root chord length [mm]

$\overline{C_w}$: Mean aerodynamic chord of wing [mm]

V_{HT} : Horizontal tail volume coefficient

l_{HT} : distance of aerodynamic center of horizontal tail to C.G. [mm]

S_{HT} : Horizontal tail surface area [mm^2]

AR_{HT} : Horizontal tail aspect ratio

b_{HT} : Horizontal tail wingspan [mm]

$C_{r_{HT}}$: Horizontal tail root chord [mm]

$C_{t_{HT}}$: Horizontal tail tip chord [mm]

$\overline{C_{HT}}$: Mean aerodynamic chord of horizontal tail [mm]

S_E : Elevator surface area [mm^2]

b_E : Elevator wingspan [mm]

C_E : Elevator mean chord [mm]

V_{VT} : Vertical tail volume coefficient

l_{VT} : Distance of aerodynamic center of vertical tail to C.G. [mm]

S_{VT} : Vertical tail surface area [mm^2]

AR_{VT} : Vertical tail aspect ratio

b_{VT} : Vertical tail wingspan [mm]

$C_{r_{VT}}$: Vertical tail root chord [mm]

$C_{t_{VT}}$: Vertical tail tip chord [mm]

$\overline{C_{VT}}$: Mean aerodynamic chord of vertical tail [mm]

S_R : Rudder surface area [mm]

b_R : Rudder wingspan [mm]

C_R : Rudder mean chord [mm]

rpm : Revolution per minute [rev/m]

rps : Revolution per second [rev/s]

M_{Total} : Total moment about the centre of gravity [gmm]

X_{cg} : Distance of centre of gravity from nose [mm]

CHAPTER 1

INTRODUCTION

1.1 General Overview

Micro Air Vehicles (MAVs) are now an active research focus that has caught attention from global talents. MAVs are classified as Unmanned Aerial Vehicles (UAVs) with dimensions not exceeding 15cm (normally corresponding to a Reynolds number less than 10^5), and an all-up maximum weight 100g, as set by the US Defense Advanced Research Project Agency (DARPA) (Mwongera, 2015). This definition however is not widely applied to all scientists, because until today there are technology limitations to produce much smaller electronics and materials for MAVs with the defined sizing. Hence, to invent MAVs that can mimic natural flyers using smallest possible manufactured parts, researchers usually do not put a strict sizing limit while designing their MAVs. With its' small size, MAVs have considerable potential to be capable of performing missions such as environmental monitoring, surveillance and assessment in hostile situation(Nakata et al., 2011). In general, there are three vehicle concepts: rotary wing, flapping wing and fixed wing as exemplified in Figure 1.1.1, Figure 1.1.2, and Figure 1.1.3.

Figure 1.1.1: Rotary MAV- MAVSTAR (Lin Chi Mak, 2009)

Figure 1.1.2: Flapping Wing MAV - DelFly Micro (G.C.H.E Decroon, 2015)

Figure 1.1.3: Fixed Wing MAV - The Black Widow (Joel M. Grasmeyer, 2001)

Figure 1..1: Three types of micro air vehicles

Fixed wing and rotary design have been observed to suffer from degraded aerodynamic performance when downsize the model (H Liu, 2011). It has been highlighted that MAVs in fixed wing designs encounter fundamental challenges in low lift-to-drag ratio and unfavorable flight control (Liu, 2011). Compared to rotary MAVs, Flapping Wing Micro Air Vehicles (FW-MAVs) are well-known for its effectively flight performance and hover capability. FW-MAVs have less payload, therefore making capable of operating in a confined environment. Also, they produced lesser noise compare to rotary design, which give them low detectability and perfect for surveillance purposes (Mwongera, 2015).

Based on inspiration of biological flyers of nature, Ornithopter type MAVs have been split into two main categories: *bird-inspired* FW-MAVs and *Insect-inspired* FW-MAVs. Both design fly by flapping their wings but fundamentally differ from each other in many ways (Shyy W, 2013) in terms of wing kinematics and control mechanisms. Insect-inspired FW-MAVs has become a rising trend for researchers to develop various prototype due to their higher degree of complexity in flight kinematics and capable of flying at low forward speed or even hovering in extremely low Reynolds number flow condition without stalling, unlike bird-inspired FW-MAVs who need an initial launching speed while flapping their wings to produce lift and propulsive thrust to fly and stays aloft in air.

1.2 Problem Statement

Through the process of mimicking insect flight, researchers from both in educational institution and industry are facing a lot of challenges such as instability of the aircraft during the hovering, the maneuverability, the propulsive efficiency due to

miniaturization and so on. To date, only a few of FW-MAVs have demonstrated untethered and controllable hovering flight. The inspiration of innovating a small but efficient FW-MAV is that, with small payload carrying capability, human can deploy FW-MAVs during environmental monitoring and indoor surveillance missions. To study and develop a kinematically stable and efficient FW-MAV with the limitations of time, budget and facilities, extensive research work and delicate hands-on skills are required. If prototype is unsuccessfully carry out the missions, the design can be improve and accordingly to make a contribution towards an autonomous control capable FW-MAV. It is important to validate the theoretical findings with experimental results using prototypes that are built. In this way, the mechanical design, flapping and control mechanisms as well as the algorithms can be improved.

1.3 Objectives

The main objective of this project is to design and develop a four-winged FW-MAV using conventional tail control mechanism for research purposes. The design goals to be achieved are summarized as follows:

1. To study the best configuration and fabrication method of wing that meet the following requirements:
    - Wingspan : less than 30 cm from left to right
    - Length : less than 30 cm (nose to tail)
    - Maximum aircraft weight : less than 40 grams
    - Endurance : minimum 5 min
    - Able to carry IMU and Barometer sensors and 4 grams of other payloads
2. To develop and manufacture a four-winged FW-MAV.

3. To conduct a flight test and study the behaviour of the FW-MAV prototype.

1.4 Thesis Layout

There are 5 chapters presented in this thesis, introduction, literature review, methodology, results and discussions and finally, conclusions and recommendation. In chapter 1 introduction, a general overview of micro air vehicles, problem statements and objectives are presented. Next, literature review of previous work, flapping mechanisms, general placement of avionics and wing sizing methods have been included in chapter 2. The next chapter is Methodology. In the beginning, the project overall methodology is reviewed followed by constraint analysis, wing and tail sizing, flapping mechanism's gear ratio and frequencies, avionics connections and prototype manufacturing methods. In chapter 4, results and discussion of the first prototype is reviewed and the centre of gravity is estimated. Besides that, flight test and vertical thrust measurement results are presented and discussed in the same chapter. The last chapter in this thesis concludes the project outcomes and future recommendations are explained.

CHAPTER 2

LITERATURE REVIEW

2.1 Previous Work

Up to date, there are only several flapping wing MAVs that can demonstrate stable hovering flight. The notable flapping wing MAVs design has been studied and presented in Figure 2.1.1 to Figure 2.1.9.

Figure 2.1.1: Harvard Robobee (Shang et al., 2009)

Figure 2.1.2: AeroVironment Humming Bird (watts et al., 2012)

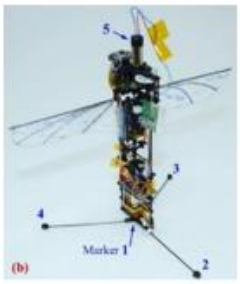

Figure 2.1.3: KUBeetle (Hoang Vu et al., 2017)

Figure 2.1.4: TL- FlowerFly (Nguyen et al., 2017)

Figure 2.1.5: eMotionButterfly (Festo et al., 2015)

Figure 2.1.6: BionicOpter (Festo et al., 2013)

Figure 2.1.7: DelFly Micro (TUDelft, 2008)

Figure 2.1.8: DelFly Explorer (TUDelft, 2013)

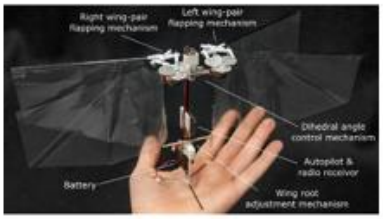

Figure 2.1.9: DelFly Nimble (Karásek et al., 2018)

Natural flyers use their wing as a lift generating mechanism to keep them stay aloft, one of the wing kinematics is Clap and Fling. The technique suggests that wings are slapped together then flung apart at the end of each stoke (Weis-Fogh, 1973). As a result, bound vortex is formed on each wing edge, which remains attached until the next stroke, thus inducing circulation on the wing, creating a pressure differential and thus encouraging high values of lift (Mwongera, 2015). Other unsteady aerodynamic mechanisms such as wing leading vertex and delayed stall (Ellington et al., 1996), wing rotation (Dickinson et al., 1999) and wake capture (Sane, 2003) are also contributing to FW-MAVs' lift generation.

In 2007, the first insect-sized FW-MAV named Harvard Robobee had been invented (Wood, 2008). Robert highlights that a high speed, highly articulated mechanisms that are necessary to replicate Insect-like wing flapping motion exist on a scale that is between microelectromechanical systems (MEMS) (Pister et al., 1992) and "macro" devices (Trimmer, 1989). Hence in his work, a "meso" scale rapid fabrication method, called smart composite microstructures (SCMs) is used to fabricate the Robobee. With only 0.06 gram and 3 cm of wingspan, this FW-MAV has achieved 3-4 minutes tethered-hovering flight with flapping frequency of 110 Hz and maximum speed of 6 m/s.

Until today, only a few research teams have successfully demonstrate controlled flight of an insect-like tailless two winged FW-MAV (Hoang Vu et al., 2017). AeroVironment have spent 5 years in a project financed by DARPA called Nano Humming Bird (Figure 2(b)), one of the few notable platforms capable of untethered hovering flight. It is regarded as a huge breakthrough in FW-MAVs research because of its gyroscopically stabilized flight without any tail control surfaces (Watts et al., 2012). Similarly KUBeetle, a 21 grams two-winged tailless aircraft flaps at a frequency of 30 Hz capable of taking off, hover and loiter (Hoang Vu et al., 2017). The most recent break

through is no tail DelFly Nimble project done by TU Delft in 2018 (Karásek et al., 2018), the MAV can hover or fly in any direction (up, down, forward, backward or sideways).

2.2 Flapping Mechanisms

Beside the conventional two-winged & tailless FW-MAVs, research institutions such as Termasek Laboratories, MAV Laboratories from TUDelft and Festo has developed hybrid FW-MAVs (from Figure 2.2.1 to Figure 2.2.4), which most of their work share a similarity of a four-winged wing con figuration.

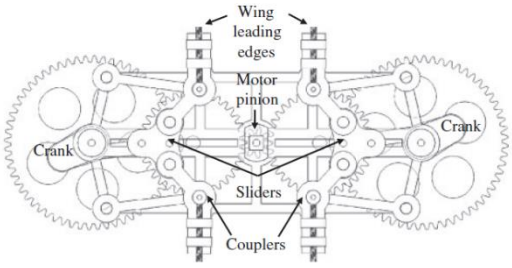

Figure 2.2.1: Four-bar linkage and pulley-string mechanism

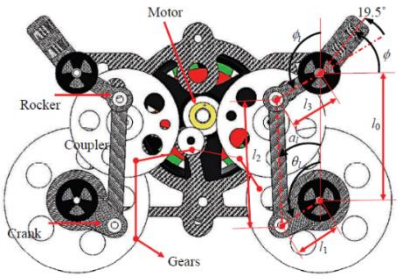

Figure 2.2.2: Four-bar linkage and crank rocker mechanism

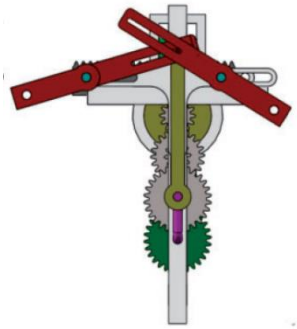

Figure 2.2.3: Crank-slider & double pendulum mechanism

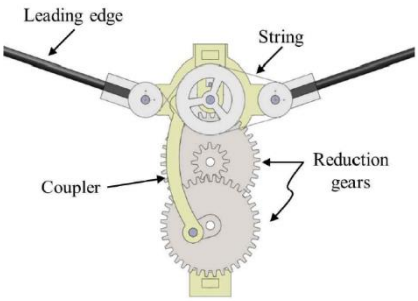

Figure 2.2.4: Two crank-slider & linkage mechanism

This wing configuration in FW-MAVs give rise to a double wing clap-and-fling effect where it has been proven that the static thrusts obtained by four wings was 30 % lager than the doubled value of those obtained by two wings for the same flapping frequencies (Kawamura et al., 2008). Tail configuration on the other hand, aircraft's conventional

tail design with control surfaces is used in most of the prototypes due to the complexity of the tailless stability control mechanism. This can be seen in the KUBeetle's feedback PD control mechanism where three sub-micro servos are used for a rotational modulation mechanism to generate necessary pitching, rolling moments (Hoang Vu et al., 2017).

There are several types of flapping mechanism being use on different FW-MAVs: pulley-string mechanism in Figure 2.2.1, crank rocker mechanism in Figure 2.2.2, crank-slider & double pendulum mechanism in Figure 2.2.3 and two crank-slider & linkage mechanism in Figure 2.2.4. From these mechanisms, it is best to use the one which requires the lesser parts for flapping movement generations, so the overall aircraft weight can be kept to its minimum. The state-of-the-art mechanisms currently are the two crank-slider & linkage mechanism using on the TL- FlowerFly (Nguyen et al., 2017) and the two four-bar linkage mechanisms using on the DelFly Nimble (Karásek et al., 2018).

The material used is one of the major key elements as it has effect on the FW-MAVs' overall performance. DelFly series and TL- FlowerFly share the similarity on the material used, where their wings are made from Mylar foil with carbon stiffeners and a D-shaped carbon rod for leading edge. Depron foam sheet is used for making the tail because of its lightweight characteristic. Highly glossy carbon fiber composite is used to fabricate the gearbox on the TL- FlowerFly for its high strength property. With these literature findings with the manufacturing capability of USM, insect-inspired FW- MAV design approach and methodology is getting visible. Although most of the FW-MAV platforms has been successfully carrying payload such as camera and sensors for control and image processing purposes, no one has tried to carry and store additional payload such as tiny speakers and LED onboard with the FW-MAVs.

2.3 General Placement of Avionics

Figure 2.3.1 (DelFly Nimble), figure 2.3.2 (KUBeetle) and figure 2.3.3 (NUS FlowerFly) reveal the location of electronics components along the fuselage in longitudinal view. In general, the flapping gearing mechanical systems and motors are always located at the nose of the aircraft. For Delfly Nimble and KUBeetle, there are also servos located at nose of the MAV for control mechanisms. These three FW–MAVs also shared a similarity which is the Autopilot, ESC and radio receivers, are located in the middle section of the fuselage, usually aft the wing structure. After that, at the rear section of the FW-MAVs, there are battery and remaining servos located. This study has provided insight into the electronics positioning on FW-MAVs. It is noted that the passive longitudinal stability can be achieved by carefully shifting the position of battery, ESC and radio receiver along the fuselage.

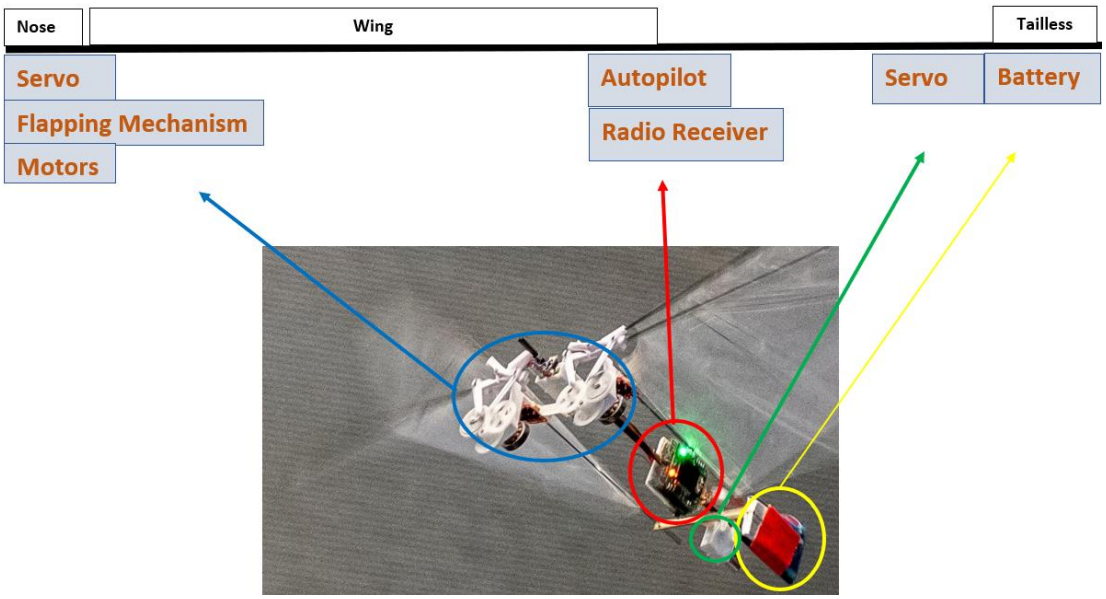

Figure 2.3.1: Electronics components location of DelFly Nimble

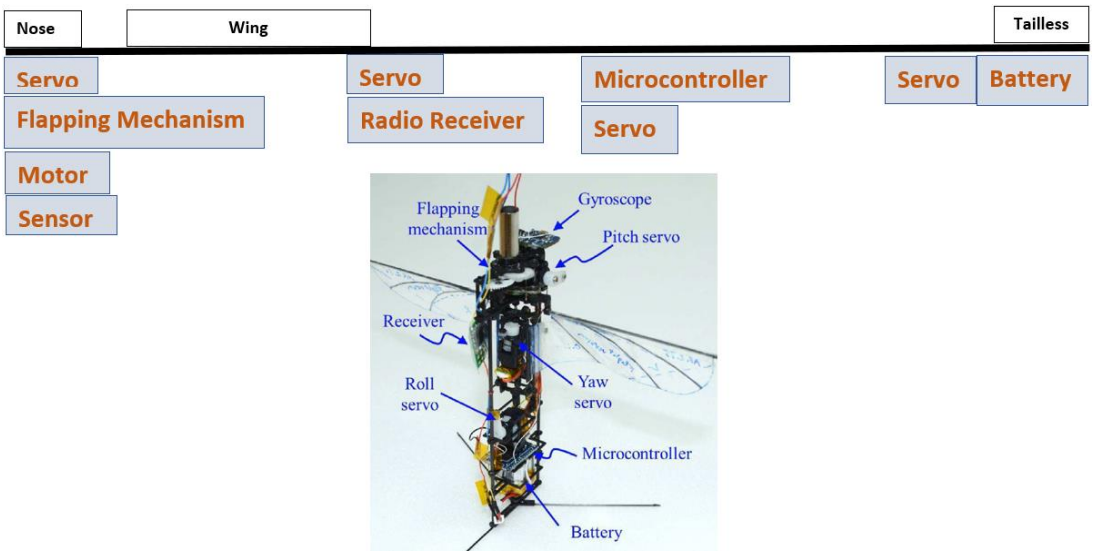

Figure 2.3.2: Electronics components location of KUBeetle

Figure 2.3.3: Electronics components location of NUS FlowerFly.

2.4 Wing Sizing Methods

There is a few of wing sizing methodology which has been used to design bio-inspired flapping wing drones. The first sizing method is generally based on empirical formulae. These formulae have related the sizing parameters and wing geometry (wing area, weight, and wing loading) to the flight performance parameters (flapping frequency, flight speed, and power required). The method has been used by some researchers

including Beasley (Beasley, 2006b). In his work, he sizes the flapping wing by utilizing the geometric scaling factors for Passeriformes where he cited from a book that had estimated the flight characteristics and body mass (Norberg, 1990). Another example, according to Mostafa (Hassanalian et al., 2016), has been applied by Gerrard and Ward, students from The University of Adelaide (Gerrard C., 2007) is based on statistical and experimental sizing and testing using existing FW–MAVs such as DelFly (De Croon et al., 2009). Until recently in year 2016, Mostafa (Hassanalian et al., 2016) claims that the MAVs designed using other methods (Gerrard C., 2007), (Whitney and Wood, 2012), (BENG, 2004), (Beasley, 2006a) are not optimized as they do not take into account the influences of other parameters such as the material used for the wing membranes(Hassanalian et al., 2016). Thus, he proposes a experimentally verified sizing method that is comprising of five steps where it includes define and analyze the FW-MAV mission, determine the flying modes, define the wing shape and aspect ratio of the wing, apply constraint analysis based on the defined mission and lastly estimate the weights of the electrical and structural components of the FW-MAV(Hassanalian and Abdelkefi, 2016). This is a theoretical, statistical methodology which is more comprehensive than other methods mentioned previously. The details of each step is explained in section 3.2.2, wing sizing methodology.

CHAPTER 3

METHODOLOGY

3.1 Project Overall Methodology

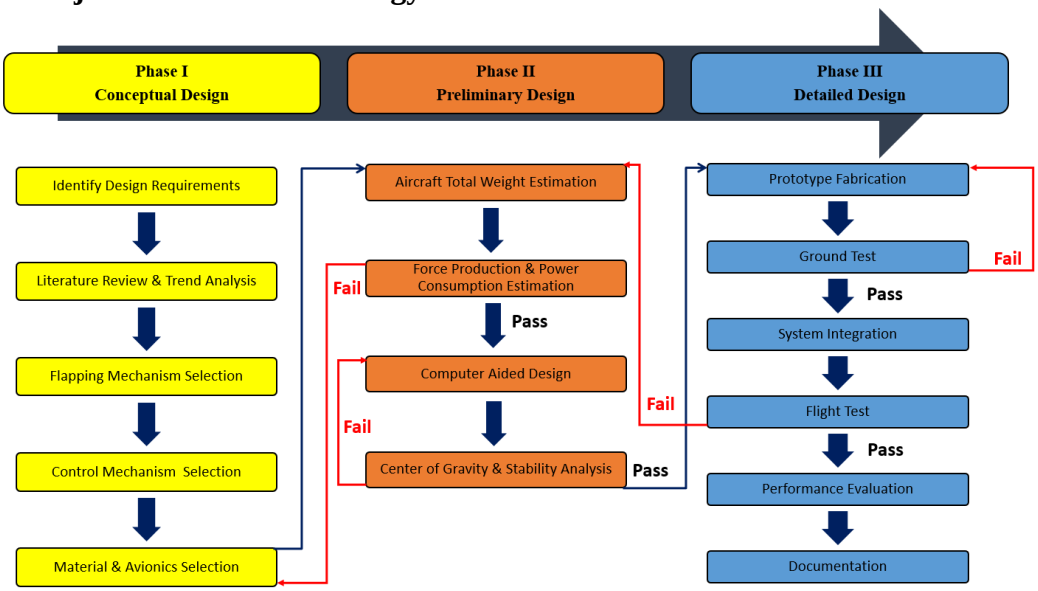

Figure 3.1.1: Overall Project Design Process

The design methodology of an Insect-inspired FW-MAV is summarized in Figure 3.1.1 where the project is divided into three main design phases. The initial phase is aircraft conceptual design, starting with identifying the design requirements for MAV such as weight, endurance, payload, wingspan and length. After understanding the needs from project stakeholder, similar work that have been done in recent 10 years will be reviewed to analyse the FW-MAVs design trend. Next, the FW-MAV flapping mechanism, control mechanism, and material selections that can contribute to a better flight performance will be finalized.

In second phase, the preliminary design will begin once the conceptual design work is finished. FW-MAVs' total weight will be estimated. Next force production will be

quoted from previous work and power consumption will be calculated. The procedure is meant to verify the FW-MAV design and see if the aircraft could lift. Once the design is proved valid, the design concept will be generated using SolidWorks to have better visualization and location of center of gravity will be determined. The FW-MAV is fabricated base on the design requirement.

Once the design is worked out and necessary materials are ready, detailed design phase will begin. Wings, flapping mechanism and control mechanism will be fabricated separately. The microcontroller, servo and other electronics will be integrated before proceeding to ground test. Ground test which includes mechanism test and electronics test will be carried out. Mechanical test mainly conducted to check the functionality of parts, for instance, examine if the wing can flap at desire frequency. On the other hand, power, radio signal and control surfaces will be tested to make sure they are working. Flight test will be carried out after the inspection of avionics connection is conducted and proved that all components are working in ground test. All parts and electronics are assembled for flight test, and the flight performance results will be analyzed to evaluate the design. Modification will be made to improve the result until the work meet the design requirements.

3.2 Conceptual Design

3.2.1 Computer Aided Design (CAD)

Throughout this project, SolidWorks is used to design and draw the 2D drawings of FW-MAVs' wing and tails, 2D and 3D drawings of MDF mold for advance wing fabrication method. The relevant drawings has been included in Appendices section of this work.

3.2.2 Wing Sizing

Step 1 – Defining the mission :

The kind of flight mission which will be carried out either indoor or outdoor has to be decided at the very beginning. In this project the FW-MAV will be flying indoor. Given the current latitude, L_0 and altitude, h_0 at Nibong Tebal, Penang, Malaysia equal to $5.4164\,°$ and 3m. Latitude and altitude value are used to calculate the acceleration of gravity at the place of flying the FW-MAV.

Based on the mission, pinpoint the relevant flight class of the flapping wing (MAV, NAV, or PAV). Then, as part of the flight planning, the mission will be analyzed including extracting the atmospheric parameters (air temperature, air density, kinematic viscosity, air pressure and acceleration of gravity) of the flight zone, determining the distances, flight time and estimating the cruise speed. These parameters will be used to calculate FW-MAV cruise speed, Reynold's Number, and other flight parameter using equations (1), (2), (3), (4) and (5).

$$g = 9.80616 - [0.025928\cos(2L_0)] + [0.000069\cos(2L_0)] - [(3.086 \times 10^{-6})h_0] \quad (1)$$

$$T_a = 15 - 0.0065h_0 \quad (2)$$

$$\rho = 1.226\left(\frac{p}{1013}\right)\left(\frac{288}{T_a + 273}\right) \quad (3)$$

$$\nu = 1.466 + 95.07h_0 + 10470{h_0}^2 \quad (4)$$

$$p = 1013\,[\,1 - (2.26 \times 10^{-5})h_0]^{5.256} \quad (5)$$

Step 2 – Defining the flight mode :

The flight modes will be determined in this step as well. Generally for an aircraft, the modes can consist of different stages including takeoff and landing, cruise flight, turning, climbing and descent flight. For FW–MAV in this project, flight modes are takeoff, forward flight, hovering, and turning.

Step 3 – Selecting the platform and aspect ratio :

After completing Step 2, the best wing shape and its aspect ratio should be selected. This can be done by studying the existing FW–MAVs' wing design and their performances with different aspect ratio. Experiments to study the effect of different wing parameters on flapping wing performance had been carried out with objectives to optimize wing shape and wing geometry for DelFly II (Nan et al., 2017) .From the study, a wing in trapezoidal shaped with aspect ratio of 3.50 tapered ratio of 0.552, and wing 8435 gives better thrust characteristics (Bruggman, 2010). Besides, it is also mentioned that wing with larger aspect ratios gained higher lift to drag ratio, which is similar to the common rules used in Fixed Wing aircrafts (Yang et al., 2017). In conclusion, the aspect ratio used for this project is 3.50 and the tapered ratio is 0.55.

Step 4 – Determining the parameter of wing loading (W/S) :

Using the atmospheric parameters in Step 1, the required flight parameters to estimate the FW-MAVs' wing loading has to be calculated in the first place. These values are used to complete the equations of thrust loading (T/W) as a function of wing loading (W/S) for different flight modes in Table 3.2.3. At this point, a constraint analysis should be conducted. Equation (6) the thrust loading (T/W) is represented as a function of wing loading (W/S). Therefore by drawing the related curves of the corresponding modes' equations, a bounden space to determine a design point (W/S, T/W) can be obtained. The

design point should satisfy all of the constraints according to the defined mission. The wing loading which satisfied all constraint will be used after Step 5 to calculate the required wing surface area.

$$\frac{\boldsymbol{T_{SL}}}{\boldsymbol{W}} = \frac{\mathbf{1}}{\boldsymbol{\alpha}}\left\{\frac{\boldsymbol{qS}}{\boldsymbol{W}}\left\{\boldsymbol{k_1}\left(\frac{\boldsymbol{n}}{\boldsymbol{q}}\frac{\boldsymbol{W}}{\boldsymbol{S}}\right)^{\mathbf{2}} + \mathbf{2}\boldsymbol{\psi}\boldsymbol{C_f}\right\} + \frac{\mathbf{1}}{\boldsymbol{U}}\frac{\boldsymbol{dZ}}{\boldsymbol{dt}}\right\} \tag{6}$$

Where, $\boldsymbol{\alpha} = \dfrac{T_a + 273.16}{T_a + 273.16 - 0.001981h_0}\left\{1 - \dfrac{0.001981h_0}{288.16}\right\}^{5.256}$

$\boldsymbol{k_1} = \frac{1}{\pi eAR}$, $e = oswald\ efficiency\ factor$

$\boldsymbol{q} = 0.5\rho {U_{ref}}^2$, $U_{ref} = local\ reference\ velocity$

$$\boldsymbol{\psi} = \frac{ratio\ of\ the\ parasite\ drag\ coefficient\ of\ flapping\ wing}{frictional\ drag\ coefficient\ for\ a\ flat\ sheet},$$

$(value\ between\ 2 - 4.4)$

$\boldsymbol{C_f} = 0.455(\log_{10} Re)^{-2.58}$

$\boldsymbol{Re} = 10^5, according\ to\ definition\ of\ MAVs$

$\boldsymbol{Z} = h + {U^2}/{2g}$

$$\boldsymbol{U} = Velocity = \frac{distance\ travelled, d}{total\ time, t}$$

The constraint equations for five different flight conditions are derived from the master equations called Mattingly's method (Nam, 2007) :

Table 3.2.1: Thrust loading equations used at different flight condition*(Nam, 2007)*

Flight Condition	Equation
Case 1 – Constant Altitude/ Speed Cruise	$\frac{T_{SL}}{W} = \frac{1}{\alpha}\left\{\frac{qS}{W}\left\{k_1\left(\frac{W}{qS}\right)^2 + 2\psi C_f\right\}\right\}$
Case 2 – Constant Climb Speed	$\frac{T_{SL}}{W} = \frac{1}{\alpha}\left\{\frac{k_1 W}{qS} + 2\psi C_f \frac{qS}{W} + \frac{1}{U}\frac{dh}{dt}\right\}$
Case 3 – Horizontal Acceleration	$\frac{T_{SL}}{W} = \frac{1}{\alpha}\left\{\frac{k_1 W}{qS} + 2\psi C_f \frac{qS}{W} + \frac{1}{g}\frac{dV}{dt}\right\}$
Case 4 – Sustained turn/ Constant turning altitude	$\frac{T_{SL}}{W} = \frac{1}{\alpha}\left\{k_1 n^2\left(\frac{W}{qS}\right) + 2\psi C_f \frac{qS}{W}\right\}$
Case 5 – Service Ceiling/ Accelerated Climb	$\frac{T_{SL}}{W} = \frac{1}{\alpha}\left\{\frac{k_1 W}{qS} + 2\psi C_f \frac{qS}{W} + \frac{1}{U}\frac{dh}{dt}\right\}$
Case 6 – Hand Launch Stall Speed	$\frac{W}{S} = \frac{1}{2}\rho U^2 C_{L_{max}}$

In the above five mentioned flight scenarios, thrust loading (T/W) has been represented as a function of wing loading (W/S). These equations is drawn using MATLAB into the same graph and a bounden space for the determination of a design point (the point that satisfy all of the constraints according to the defined mission and also provide the maximum possible wing loading and minimum thrust loading).

Step 5 – Estimating the electrical and structural weights of FW - MAV :

It is important to estimate the FW-MAVs' weight with minimum error. In this project, structural mass and electrical components mass is estimated separately using Shimadzu micro weighing scale ATY 224.

Defining the weight of the structure by W_{Str} and the weight of the equipment by W_{Eq}. The total weight of the FW–MAV can be expressed as :

$$W_{To} = W_{Eq} + W_{Str} \quad (7)$$

The weight of the electrical components, W_{Eq} can be written as follows:

$$W_{Eq} = W_B + W_{PL} + W_{AV} + W_{PP} \quad (8)$$

Where W_B denotes the weight of the battery, W_{PL} represents the weight of payload, such as sensors, cameras, and additional loads for extra payload to be carried onboard in future. W_{AV} is the weight of the avionic system including servo motors, receiver and micro controller and lastly W_{PP} represents the weight of the power plant which consists of the motor and ESC. Next, the weight of the structure, W_{Str} is expressed as :

$$W_{Str} = W_{Wing} + W_{Tail} + W_{Fuselage} + W_{Mechanism} + W_{Other} \quad (9)$$

W_{Wing} is the total weight of the wing that includes the wing structure (leading edge spars and stiffeners) and the wing membrane. W_{Tail} and $W_{Fuselage}$ are denotes weight of tail and weight of fuselage. As for the weight of the flapping mechanism ($W_{Mechanism}$), it consists of the weight of gearbox system, linking bars, joints and parts connecting to the wing structure. W_{Other} is generally defined for weight of other parts such as landing gear which is not available in this project.

Since the weight of the electrical components can be estimated using equation (8), the only weight that is remaining unknown is the weight of the structure. Here, a statistical method is used to estimate the FW-MAV structure weight by using statistical data extracted from different references (Silin, 2010),(Hassanalian and Abdelkefi, 2016). From Table 4, there are three distinct group to be considered according to the weight of FW-MAV. Each of the weight constituent in percentage for these group is presented.

Table 3.2.2 : Percentage of the weight of the constituents of flapping wings for the three weight classes *(Hassanalian and Abdelkefi, 2016)* .

Weight Range (g)	$W_{PP}(\%)$	$W_{PL}(\%)$	$W_B(\%)$	$W_{AV}(\%)$	$W_{Str}(\%)$
< 100	23	2	24	13	38
100 – 400	16	1	14	9	60
400 – 800	12	0	12	4	72

In this project we will consider the weight range that is less than 100g. Notice that we can estimated the structure weight of the FW-MAV using the percentage reference which is 38%. After that, the total weight of FW-MAV can be estimated using equation (7). After the total weight and the wing loading values are obtained from step 4, the total wing area can be calculated using equation (10).

$$S_w = \frac{W_{TO}}{Wing\ loading\ obtained\ (step\ 4)} \tag{10}$$

Thus, the wing span, wing mean chord, root chord and tip chord for the wing can be calculated using equations (11) and (12):

$$AR = \frac{b^2}{S_w} = \frac{b}{\overline{C_w}} \tag{11}$$

$$Tapered\ Ratio = \lambda = \frac{C_t}{C_r} \tag{12}$$

3.2.3 Tail Sizing

Horizontal Tail Sizing

To size the horizontal tail, the mean aerodynamic chord of the wing, $\overline{\boldsymbol{C_w}}$ and the distance of mean aerodynamic center of the horizontal tail to C.G., l_{HT} has to be calculated in advance (Ozgen, 2015). The mean aerodynamic chord can be calculated using equation (13) which quoted from (JD Anderson, 1999) :

$$\boldsymbol{M.A.C.} = \overline{\boldsymbol{C_w}} = \frac{2}{3} \times C_r \times \frac{(1 + \lambda + \lambda^2)}{(1 + \lambda)} \tag{13}$$

The typical horizontal tail volume coefficient, $\boldsymbol{V_{HT}}$ is between 0.30 to 0.60 (Zumwalt, 2016). A value in between the range is selected. Using the values above, the horizontal tail surface area , S_{HT} can be calculated using equation (14) (Ozgen, 2015):

$$\boldsymbol{V_{HT}} = \frac{l_{HT} S_{HT}}{S_W \overline{C_w}} \tag{14}$$

Aspect ratio of tail has to be lower compared to the wings (Ozgen, 2015). This is because when the wing stalls, horizontal tail will still have attached flow and control authority Since the tail aspect ratio and horizontal tail surface area is available, the next step is to calculate the horizontal tail wingspan, b_{HT} , mean horizontal tail length, C_{HT} , horizontal tail root chord, $C_{r_{HT}}$ and horizontal tail tip chord, $C_{t_{HT}}$ using equation (15) to (17):

$$AR_{HT} = \frac{\boldsymbol{b_{HT}}^2}{S_{HT}} \tag{15}$$

$$\boldsymbol{S_{HT}} = \frac{1}{2} \times (C_{r_{HT}} + C_{t_{HT}})(\frac{b_{HT}}{2}) \times 2 \tag{16}$$

$$\overline{\boldsymbol{C_{HT}}} = \frac{1}{2} \times \left(C_{r_{HT}} + C_{t_{HT}}\right) \tag{17}$$

To determine the horizontal tail root chord length and tip chord length, a tapered ratio which is similar to the wing is used (Ozgen, 2015):

$$Tapered\ ratio = \frac{C_{t_{HT}}}{C_{r_{HT}}}$$

Finally, to determine the elevator control surface sizing, that ratio of elevator surface area to horizontal tail surface area and the ratio of elevator span to horizontal tail span have to be determined. The typical elevator volume is 25-33% of the horizontal tail volume (Zumwalt, 2016). It is noted that the elevator area must not be too small to avoid difficulty in stall recovery. As for the elevator span , it is best to keep span length 80-90% of the horizontal tail span length (Ozgen, 2015). These ratios will be used to size the elevator using equations (18) and (19):

$$\boldsymbol{S_E = ratio\ of\ elevator\ area\ to\ horizontal\ tail\ area \times S_{HT}} \quad (18)$$

$$\boldsymbol{b_E = ratio\ of\ elevator\ span\ to\ horizontal\ tail\ span \times b_{HT}} \quad (19)$$

Vertical Tail Sizing

In general, the same method is used to size the vertical tail and rudder (Ozgen, 2015). However, The typical vertical tail volume coefficient, $\boldsymbol{V_{HT}}$ has a range of 0.05 to 0.10 (Kamaruddin, 2017). Using the best value suggested, the vertical tail surface area can be calculated using equation (20):

$$\boldsymbol{V_{VT}} = \frac{l_{VT} S_{VT}}{S_W b} \quad (20)$$

The same value of Aspect ratio with the horizontal tail is used to calculate the vertical tail wingspan, b_{VT}, mean vertical tail length, C_{VT} , vertical tail root chord, $C_{r_{VT}}$ and vertical tail tip chord, $C_{t_{VT}}$:

$$AR_{VT} = \frac{\boldsymbol{b_{VT}}^2}{S_{VT}} \quad (21)$$

$$\boldsymbol{S_{VT}} = \frac{1}{2} \times (C_{r_{HT}} + C_{t_{HT}})(\frac{b_{HT}}{2}) \times 2 \quad (22)$$

$$\overline{\boldsymbol{C_{VT}}} = \frac{1}{2} \times \left(C_{r_{VT}} + C_{t_{VT}}\right) \tag{23}$$

$$\boldsymbol{S_{VT}} = \overline{\boldsymbol{C_{VT}}} \times \boldsymbol{b_{VT}}$$

The typical rudder volume is 25-33% of the horizontal tail volume (Zumwalt, 2016) which is the same as the elevator. It is best to keep span length 80-90% of the horizontal tail span length (Ozgen, 2015). These ratios will be used to size the rudder using equations (24) and (25):

$$\boldsymbol{S_R = ratio\ of\ rudder\ area\ to\ horizontal\ tail\ area \times S_{VT}} \tag{24}$$

$$\boldsymbol{b_R = ratio\ of\ rudder\ span\ to\ horizontal\ tail\ span \times b_{VT}} \tag{25}$$

3.2.4 Crank-Shaft Mechanism's Gear Ratio

According to Bart Bruggeman in his master thesis (Bruggeman, 2010), The gear ratio (GR) is a parameter used to define the relation between the number of teeth of two connecting gears. Using the same reference, the gear ratio of the crank-shaft mechanism can be calculated. The motor pinion has 7 teeth and it is connected to second gear which possess 40 teeth. Here, the first gear ratio, GR_1 for this two gears is therefore $\frac{40}{7}$. Noticed that there is another 9 teeth pinion gear on second gear where it is connected to the main gear which has 40 teeth as well. The second gear ratio, GR_2 for this pair of gears is $\frac{40}{9}$. The overall gear ratio for the crank-shaft mechanism, $GR_{Mechanism}$ can be calculated by multiplying the GR_1 and GR_2 shown in equation (26):

$$\boldsymbol{GR_{Mechanism}} = GR_1 \cdot GR_2 \tag{26}$$

3.2.5 Flapping Frequencies

To estimate the frequency range of FW–MAV in this project, the motor KV, battery's voltage and the gear ratio have to be identified. The motor used in this project is taken from the flapping bird model, the specification of the motor can be found in Appendix E. The motor turns 35000 rpm for 3.7 volt of voltage supply. The battery voltage is 3.7V. Gear ratio has been calculated in section 3.2.4. By dividing motor turn rate per second by the overall gear ratio, the FW–MAV flapping frequency can be calculated.

$$\boldsymbol{Frequency} = \frac{\boldsymbol{Motor\ revolution\ per\ second}}{\boldsymbol{Gear\ Ratio}} \tag{27}$$

The experimental result (Nguyen et al., 2017) shows that as the flapping frequency increases, the vertical thrust produce by the wing will also increase. It is believed that at frequency 17.3 Hz, the vertical thrust generation can go higher and enable the FW-MAV to takeoff and hover. The vertical thrust for one flapping cycle is shown in Figure 3.2.5.1 and the maximum flapping frequency and vertical thrust for different wing configurations is shown in Figure 3.2.5.2.

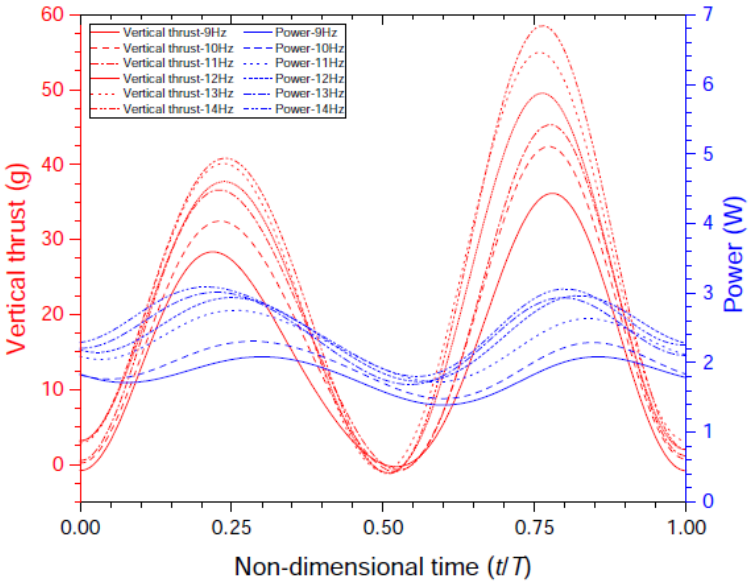

Figure 3.2.5.1: Time-dependent vertical thrust of Wing#3 for various frequencies (Nguyen et al., 2017).

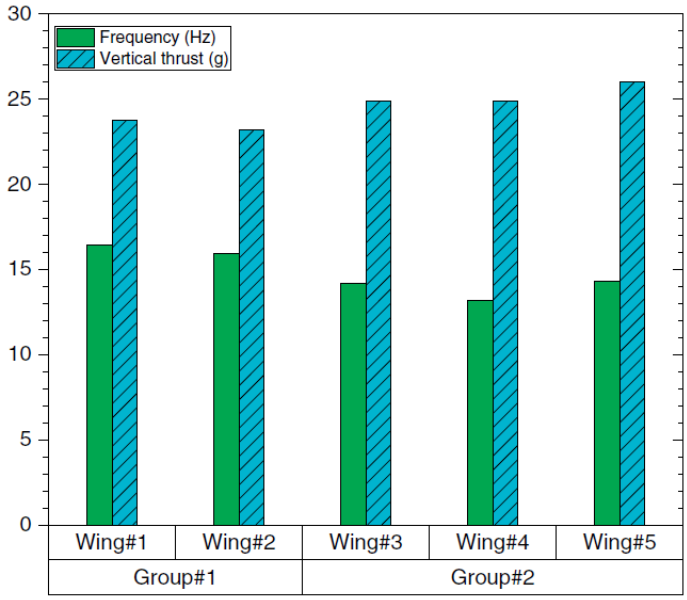

Figure 3.2.5.2: Maximum flapping frequency and vertical thrust of various wing configurations at full throttle level from the radio transmitter (Nguyen et al., 2017).